Combustible linings and room fire growth - a first analysis

Magnusson, Sven Erik; Sundström, Björn

1985

ND UNIVERSITY · SWEDEN
STITUTE OF SCIENCE AND TECHNOLOGY
EPARTMENT OF FIRE SAFETY ENGINEERING
PORT LUTVDG/(TVBB-3030)
SN 0282-3756

VEN ERIK MAGNUSSON · BJÖRN SUNDSTRÖM

OMBUSTIBLE LININGS AND ROOM FIRE ROWTH – A FIRST ANALYSIS

ND 1985

search project financed by the Swedish Fire Research Board (BRANDFORSK)

B Mass transfer number
c Specific heat
h Heat transfer coefficient (total)
k Thermal conductivity
L Heat of vaporization
$\dot{m}''$ Mass loss rate
$\dot{Q}''$ Rate of heat release per unit area ($\dot{Q}''$ without subscript refers to rate of heat release from small-scale test)
$\dot{q}''$ Rate of heat transfer per unit area
r_{ox} Mass oxygen/fuel stoichiometric ratio
T Temperature
Y_{o_2} Mass fraction of (oxygen) O_2
α Undetermined parameter in Eq 22
α' $\ell n\alpha$
β Undetermined parameter in Eq 22
ϵ Absorptivity of surface
θ Temperature rise
λ Rate of heat release curve decay coefficient
ρ Density
χ Degree of complete combustion
ΔH Heat of combustion

Subscript

a Ambient
av Average
b Burning
c Convective
e Externally impressed
f Flame
p Pyrolysis of ceiling
rt Room test
s Surface
uf Unburnt fuel reaching ceiling

The compartment fire growth and fire spread has been a subject of extensive investigations, experimental and theoretical, during the last decade. For the case when the burning item is an isolated or single object such as a bed, an upholstered chair, etc, research has on the whole been successful and given a quantitative understanding of the physical phenomena involved. Room fire growth on combustible linings remains a virtually unexplored area, despite the fact that this has been a problem of concern to the legislators and authorities since the advent of building fire safety regulations. As a consequence,

there still exists no internationally accepted basis for a functional classification of surface finishes.

The work in this area can be divided into three interacting lines of development. The first concerns the generation of improved small-scale test methods. From an international, and perhaps especially European, point of view the work carried out within the International Organization for Standardization (ISO) is of importance as it opens the way for the replacement of the multitude of national test standards with internationally agreed ones. The second line of development relates to the development of a full-scale room test procedure, initiated within ASTM and taken up by ISO. The third trend concerns the evolution of mathematical modelling, both of the fire process in the small-scale laboratory apparatuses and the full-scale fire growth.

These three lines give the structure of the Swedish research project that is the subject of this paper.

Regarding the extensive work carried out within ISO in order to generate tests for measuring "reaction to fire" of building materials, Refs *1* and *2* give a general review of the historical background, the philosophy of hazard assessment by testing methods, and the possible use of specific tests to derive material flammability characteristics for use in fire environment modelling.

Objective and Extent of the Project

The objectives of the project were threefold: to utilize the proposed ISO tests to derive basic flammability characteristics which could rationally be used as classification criteria; to generate a full-scale fire test standard; and, finally, to mathematically correlate small-scale test data and the full-scale fire process. For this purpose, 13 materials were tested in eight small-scale tests in the full-scale test room and in a one-third scale version of this room. Table 1 lists the materials and Table 2 the test methods. The project is part of a larger one, described in Ref *3*, carried out jointly by the Swedish National Testing Institute and Lund Institute of Technology.

Full-Scale Test

The full-scale test room [*4*], built at the Swedish National Testing Institute, is a lightweight concrete construction with dimensions and instrumentation according to the proposed ASTM standard room fire test [*5*]. Rate of heat release is measured by the oxygen consumption method. The test room has been extensively calibrated with results indicating that the total inaccuracy of the system is within 25 kW or $\pm 10\%$ of the measured value. In the full-scale test series, the material was mounted on the ceiling and all walls except the doorway wall. The material was ignited with a 0.17-m^2 propane sand burner located in one corner of the test room. During the first 10 min of an experiment, the gas burner heat output was kept at 100 kW, which produced a

TABLE 1—*Tested materials.*

No.	Type	Thickness, mm	Weight
1	Insulating fiberboard	13	250 kg m^{-3}
2	Medium density fiberboard	12	600 kg m^{-3}
3	Particleboard	10	750 kg m^{-3}
4	Gypsum plasterboard	13	700 kg m^{-3}
5	Polyvinyl chloride (PVC) wall covering on gypsum plasterboard	0.7	240 g m^{-2}
6	Paper wall covering on gypsum plasterboard	0.6	200 g m^{-2}
7	Textile wall covering on gypsum plasterboard	0.7	370 g m^{-2}
8	Textile wall covering on mineral wool	50[a]	100[a] kg m^{-3}
9	Melamine-faced particleboard	1.2	810[b] kg m^{-3}
10	Expanded polystyrene	50	20 kg m^{-3}
11	Rigid polyurethane foam	30	30 kg m^{-3}
12	Wood panel, spruce	11	530 kg m^{-3}
13	Paper wall covering on particleboard	see Material No. 6	

NOTE—The wall coverings were glued on the substrates (similar types as Materials 2-4) according to the manufacturers' instructions. The expanded polystyrene was glued on 10-mm-thick calcium silicate board.

[a] Refers to mineral wool.

[b] Density of entire product.

TABLE 2—*Range of material tests used in the investigation.*

No.	Tested Method Designation	Reference
1	ISO ignitability	*11*
2	ISO surface spread of flame	*1*
3	Surface spread of flame	*10*
4	RHR apparatus	*15*
5	Sensenig apparatus	*16,17*
6	Cone calorimeter	*24*
7	Swedish box test	
8	NBS smoke density chamber	
9	1/3-model-scale room	
10	Full-scale room	*5,4*

NOTE—IMO = International Maritime Organization; OSU = Ohio State University; STFI = Swedish Institute for Wood Research; RHR = Rate of Heat Release.

flame that reached the ceiling. If flashover did not occur, the heat output was then increased to 300 kW and the experiment was discontinued after another 10 min.

Figure 1 gives the heat release curve for Material 3.

Methods of Analysis

When analyzing the full-scale data and the correlation to bench tests results, several methodologies are possible. These methodologies include a

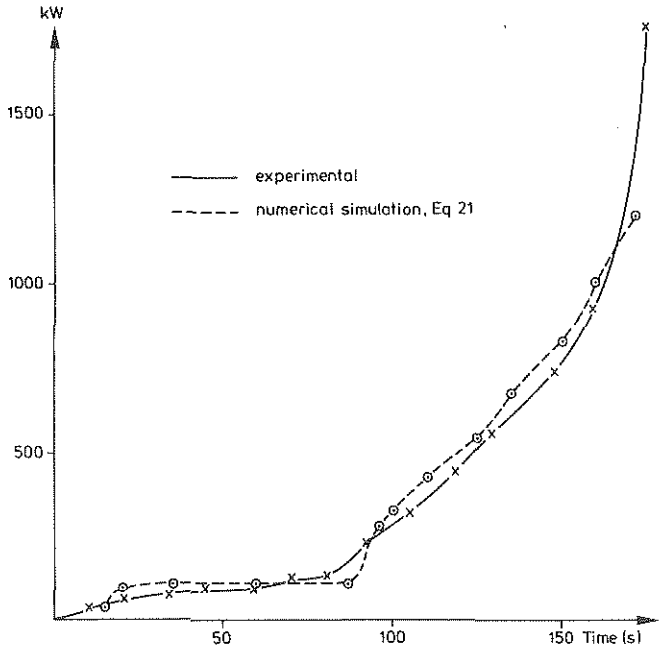

FIG. 1—*Full-scale energy release rate, experimental (full line) and numerical simulation (broken line), Eq 21.*

statistical factor analysis, a statistical modelling of the full-scale test process using regression analysis, deterministic modelling using the zone-volume approach, the field equation methodology, scale modelling, etc. We will in this preliminary report concentrate on the second method, leaving other approaches to future papers.

The different approaches reflect the degree of knowledge we have of the physical processes. The factor analysis method is of the "black box" type; typical discrete events in the fire growth (time to 500 kW, time to flashover, etc.) are described as a function of the independent variables such as ignition source output and $k\rho c$ of lining material. Nothing is assumed known of the fire growth phenomenon. The second method assumes that the basic structure of the model is understood and that unknown parameters in the model can be estimated by regression analysis. Deterministic zone modelling requires a more detailed knowledge of component processes, etc.

The reason for concentrating the initial efforts on statistical regression analysis is that this procedure promises to be the fastest way of obtaining a

design equation or design procedure; albeit they may be approximate, empirical, and temporary ones.

Basic Regression Model

The scenario we are considering is the following one: The walls and the ceiling of the test room are lined with the material. The ignition source in the corner ignites the wall corner material and spreads upward on an area approximately equal to 0.7 m^2, equal to the width of burner (0.17 m) times the distance from the burner to the ceiling. The flame from the 100-kW ignition source has such size that upward spread and involvement of the wall corner area can be considered as nearly instantaneous, which considerably simplifies the analysis. The resulting ceiling jet or flame spreads along the intersections between the walls and ceiling and along the ceiling area in the mode of concurrent flame propagation. The model is primarily intended to describe this phase of the fire growth. After a certain time delay, flames begin to spread vertically downward from the ceiling and horizontally from the burning corner plume area. The mode of the flame spread is here "creeping" or opposite the air flow direction.

Our model will be based on the concepts presented in Refs *6–8*. It is demonstrated in these references that for the ceiling flame spread and combustion:

1. Flame area A_f is linearly increasing with the total rate of heat production, that is, with the ceiling pyrolysis area A_p

$$A_f = c_1 A_p \tag{1a}$$

2. Subsequent pyrolysis areas A_p are proportional to the initial pyrolyzing area $A_{p,o}$

$$A_p \sim A_{p,o} \tag{1b}$$

3. The rate of spread of A_p is inversely proportional to the time δt necessary to increase the surface temperature at the flame tip from an initial temperature T_a to a pyrolysis temperature T_p.

From the results just enumerated, it follows that A_p may be considered as a driving force in a process where the rate of increase of A_p is proportional to the quantity A_p itself

$$\dot{A}_p \approx \frac{A_f - A_p}{\delta t} = \frac{c_1 - 1}{\delta t} A_p \tag{2}$$

with δt as just defined; that is, A_p is exponentially increasing with time. For the quantity δt and a thermally thick material, the following expression is given by elementary heat conduction theory

$$\delta t \sim k\rho c(T_{ig} - T_a)^2/\dot{q}''^2 \tag{3a}$$

where

T_{ig} = the ignition temperature,
T_a = the ambient temperature,
$k\rho c$ = the product of thermal conductivity k and thermal capacity ρc, and
$\dot{q}''$ = effective net heat flux from flame to ceiling.

$\dot{q}''$ can be formally written as

$$\dot{q}'' = h(T_f - T_a) \tag{4}$$

where

h = total heat transfer coefficient, and
T_f = flame temperature,

and consequently

$$\delta t \sim k\rho c(T_{ig} - T_a)^2/[h(T_f - T_a)]^2 \tag{3b}$$

The nondimensionalized time

$$h^2 t/k\rho c \equiv at \tag{5}$$

is thus an important scaling parameter.

From Eqs 2 and 3*b*

$$\dot{A}_p \sim aA_p \tag{6}$$

It follows that in a regression model of ceiling flame spread and combustion, pyrolysis area A_p can be generally written as

$$A_p = f(e^{at}) \tag{7}$$

One possibility is to write

$$A_p = \alpha(e^{at} - 1)^\beta \tag{8}$$

where α and β are coefficients to be determined statistically. Equation 8 will be the basic equation for the regression analysis.

The experimental variable from the room test used to validate the model is rate of energy release, $\dot{Q}_{rl}$. If we define $\dot{Q}_{cv}$ as that part of $\dot{Q}_{rl}$ that derives from ceiling combustion, $\dot{Q}_{cv}$ is written

$$\dot{Q}_{cv} = A_p \dot{Q}''_{av} \tag{9}$$

where $\dot{Q}''_{av}$ is a suitable time and space averaged measure of material rate of heat release per unit area.

The next sections will be devoted to find values of $k\rho c$ and $\dot{Q}''_{av}$ to use in Eqs 8 and 9.

Basic Flammability Parameters

Various lists of these parameters have been published. An example is the analysis in Ref *9*, which concludes with the following enumeration:

1. Thermal inertia $\sqrt{k\rho c}$.
2. "Creeping" flame spread coefficient C.
3. Minimum radiant flux for ignition $\dot{q}''_{o,ig}$.
4. Minimum radiant flux for flame spread $\dot{q}''_{o,s}$.
5. Heat of reaction ΔH.
6. Stoichiometric oxygen to fuel ratio r_{ox}.
7. Heat of vaporization L.

The first four are parameters needed in the analysis of room fire ignition and flame spread, while the last three, as will be discussed later on, are applicable to a description of rate of energy release. Because of the full-scale room test scenario and choice of regression model, we will concentrate our discussion on the results obtained from the ignitability and rate of heat release apparatuses (Methods 1,4,5 in Table 2). As mentioned, the full-scale experiment design assumes that the lining material covers walls *and* ceilings. Obviously, in real life situations a common practice is to put lining only on the walls. For this case, the modelling will have to be based on parameters derived also from the "creeping" surface spread of flame test methods analyzed in Ref *10* (Parameters C, $\dot{q}''_{o,ig}$, and $\dot{q}''_{o,s}$ in the just-mentioned list).

Ignitability Test and Derivation of $k\rho c$

The test—ISO TC92 TR5657, Fire Tests, Reaction to Fire, Ignitability of Building Products—is described in Ref *11*.

The test is performed by exposing horizontal specimens to constant irradiance $\dot{q}''_e$ at specified levels ranging from 10 to 50 kW/m^2. The irradiance is provided by an electrically heated radiator cone positioned above the speci-

men. The cone has a hole at the top to avoid trapping any combustible gases. A pilot flame is applied once every 4 s to a position 10 mm above the surface of the specimen to ignite any volatile gases.

The specimen is placed on a silicate baseboard, and a counterweight system ensures that the specimen is kept in position and receives constant heat flux during the test.

Five replicate tests were performed on each irradiance level, 10, 20, 30, 40, and 50 kW/m^2.

Although not included in the normal test procedure, thermocouples were attached to the sample surface and between the sample and the baseboard, recording the temperature rise at these locations.

The main quantitative information obtainable from the ISO ignitability test is a set of values of t_{ig}—ignition time—for a set of exposure radiation levels $\dot{q}_e''$. The ignition time values can be regarded as relative hazard indices in themselves. Methods of deriving the indices are suggested in Refs *11* and *12*. Data also can be extrapolated to yield useful quantities such as minimum level of impressed flux to cause ignition. Finally, and with the supplementary temperature measurements described earlier, test output can be used to derive important material and process parameters such as thermal conductivity k and thermal capacity ρc of the tested specimen. A prerequisite is a model of the test process.

A substantial effort was made to investigate available approaches to derive $k\rho c$. These approaches included various forms of analytical modelling and use of nonlinear regression methods and are described in some detail in Ref *13*. In the end it was found that the most practical way of calculating $k\rho c$ was to use an approximate integral solution derived in Ref *14*, giving the surface temperature rise θ_s from the relation

$$t = U\left[\frac{\theta_s^2}{\dot{q}''} + \frac{\tau}{\gamma^{3/2}} \ln \frac{(2s\theta_s + \tau - \sqrt{\gamma})(\tau + \sqrt{\gamma})}{(2s\theta_s + \tau + \sqrt{\gamma})(\tau - \sqrt{\gamma})} - \frac{\theta_s(\tau + 2s\theta_s)}{\gamma \dot{q}_e''}\right] \quad (10)$$

where

$$U = \frac{2}{3}\frac{k\rho c}{\epsilon^2} \quad (11a)$$

$$\tau = -(h_c/\epsilon + 4\sigma T_a^3) \quad (11b)$$

$$s = -\frac{25}{3}\sigma T_a^2 \quad (11c)$$

$$\gamma = (\tau^2 - 4\dot{q}_e'' s) \quad (11d)$$

and

$$\dot{q}_e'' = \dot{q}_e''/\epsilon = \dot{q}_e'' + \tau\theta_s + s\theta_s^2 \qquad (11e)$$

$\dot{q}_e''$ is the impressed flux and ϵ the absorptivity of surface.

Equation 10 demonstrates the invariate or scaling properties of the factor $t/k\rho c$. The Eqs 10-11 constituted the basis for experimental determination of $k\rho c$.

It was found that the calculated $k\rho c$ will vary with time (which strictly speaking invalidates the theory behind Eqs 10-11) but not excessively. Typical examples are given in Fig. 2. The average values of $k\rho c$ used in subsequent calculations are given by Table 3.

Rate of Heat Release (RHR) Measurements and Characteristics

The 13 materials have been tested in three different RHR apparatuses: the Ohio State University apparatus [*15*], an open configuration [*17*] based on a design originally developed by National Bureau of Standards (NBS) [*16*], and the cone calorimeter [*18*]. The analysis made in this report will be based on the measurements reported in Ref *17*.

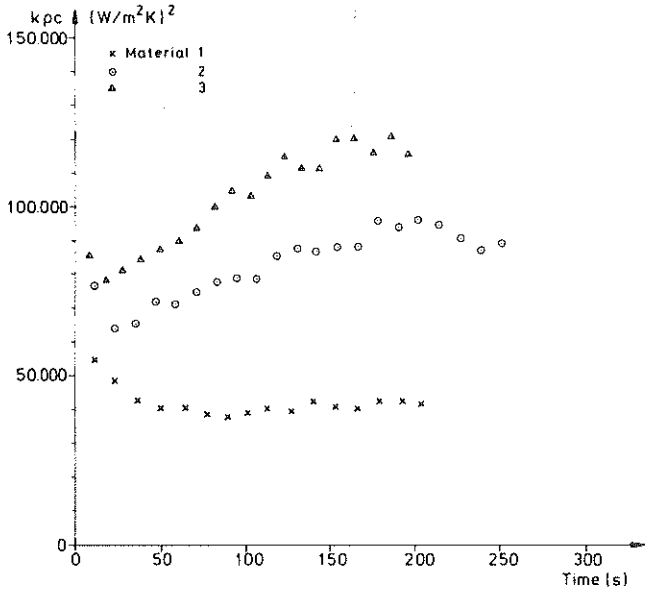

FIG. 2—kρc *values obtained from Eq 10 for three materials.*

TABLE 3—*Derived material properties.*

Mat No.	$k\rho c \times 10^{-3}$ $(W/m^2\ K)^2$	$\dot{Q}''_{max}$, kW/m^2	λ, s^{-1}
1	41	139.8	0.0070
2	80	162.4	0.0027
3	110	199.8	0.0049
4	100	27.7	0.0150
5	75	107.5	0.0293
6	100	105.3	0.0208
7	80	222.0	0.0278
8	4.3	246.2	0.0382
9	105	40.9	−0.0032
10	...	...	...
11	4.0	130.6	0.0217
12	85	149.7	0.0086
13	110	164.1	0.0035

The equipment consists of a vertical sample holder and an electrical radiation panel placed under an open hood.

The samples were tested at 5, 3, and 2 W/cm^2 and some easily ignitable materials also at 1 W/cm^2. Three examples of test output are given in Figs. 3*a*, 3*b*, and 3*c* for Materials 3, 7, and 8 (compare Table 1).

Formally, the mass loss rate $\dot{m}''_b$ from a burning surface may be written

$$\dot{m}''_b = \frac{1}{L}\dot{q}''_{net} \tag{12}$$

where $\dot{q}''_{net}$ is the difference between heat flux to the fuel surface (externally applied flux, flux from flames) and heat loss terms (radiative and convective loss from the surface, heat conducted into the bulk of the fuel, cooling agents applied). L may be defined as the heat required to produce volatiles. If we accept Eq 12 in a formal sense, then $\dot{Q}''$ is given by

$$\dot{Q}'' = \chi\Delta H\dot{m}''_b = \chi\frac{\Delta H}{L}\dot{q}''_{net} \tag{13}$$

where χ stands for degree of combustion completeness. Obviously, the quantity $\Delta H/L$ is a parameter of major importance. It is also a component in the mass transfer number B, which plays a fundamental role in the theory of convection-controlled combustion. An engineering approximation to B is given by the expression

$$B = \frac{\Delta H}{L} r_{ox} Y_{o,a} \tag{14}$$

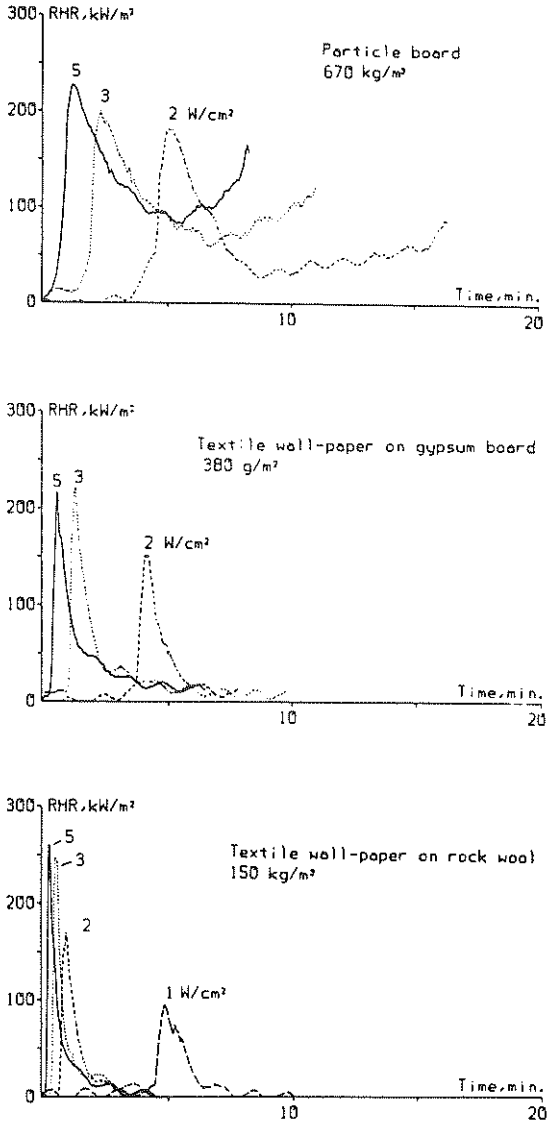

FIG. 3—*Experimental RHR curves for Materials 3, 7, and 8.*

where

r_{ox} = mass oxygen to fuel stoichiometric ratio, and
$Y_{o,a}$ = ambient mass fraction of oxygen.

As described in Ref *13*, the initial attempt was to try to derive the parameters ΔH, L, and r_{ox} from the RHR curves exemplified by Fig. 3. Unfortunately, it turned out that transient effects (the bulk heating term) made calculation of L unreliable. The longer heating-up period before ignition at lower flux levels in some cases neutralizes the effect of higher levels of external flux on rate of mass loss. There was also a considerable scatter in the computed values of ΔH and r_{ox}. As a consequence, it was decided to describe and make use of the RHR characteristics of the involved material directly, using a mathematical approximation of the curves shown in Fig. 3, primarily the curves valid for an external flux equal to 30 kW/m^2. In the full-scale experiments, heat fluxes to the lining material will vary considerably with time and location. A study of available literature indicated that an average value of 30 kW/m^2 might be more representative than 50 kW/m^2, but this has not been substantiated.

The experimental curves were idealized in the following way (Fig. 4). After exposure at $t = 0$, the sample will gradually heat up and reach pyrolysis temperature T_p at $t = t_p$. The mass loss rate during this period is neglected. At $t = t_p$, pyrolysis and rate of heat release jump to a maximum value $\dot{q}''_{\max}$ and start to decay. Asymptotically, the rate of pyrolysis is proportional to $(t - t_p)^{-1/2}$ [*19*]. For the initial transient period, which is of main interest for room fire growth process, it was found suitable to write

$$\dot{Q}''(t) = \dot{Q}''_{\max} e^{-\lambda(t - t_p)} \tag{15a}$$

or, alternatively

$$\dot{Q}''(t) = \dot{Q}''_a + (\dot{Q}''_{\max} - \dot{Q}''_a) e^{-\lambda(t - t_p)} \tag{15b}$$

Here we will exclusively use Eq 15*a*. The $\dot{Q}''_{\max}$ values were taken directly from measurement and can be found together with the corresponding regression values of λ in Table 3. Figure 5 shows experimental curves and approximations according to Eq 15*a* for Materials 3, 7, and 8.

For the products investigated in this project, with the exception of Materials 9 and 10, the expression (Eq 15*a*) seemed phenomenologically correct. Thermoplastics like polystyrene, which melt and drip away before and after ignition, behave in such a way that modelling seems a remote possibility. Indeed, the room test was at least partly motivated by the incapability of small-scale tests to rationally evaluate the flammability characteristics of these materials. For Material 9, which is a composite, the general appearance of the small-scale test RHR curves varies with level of impressed flux, with the 30-

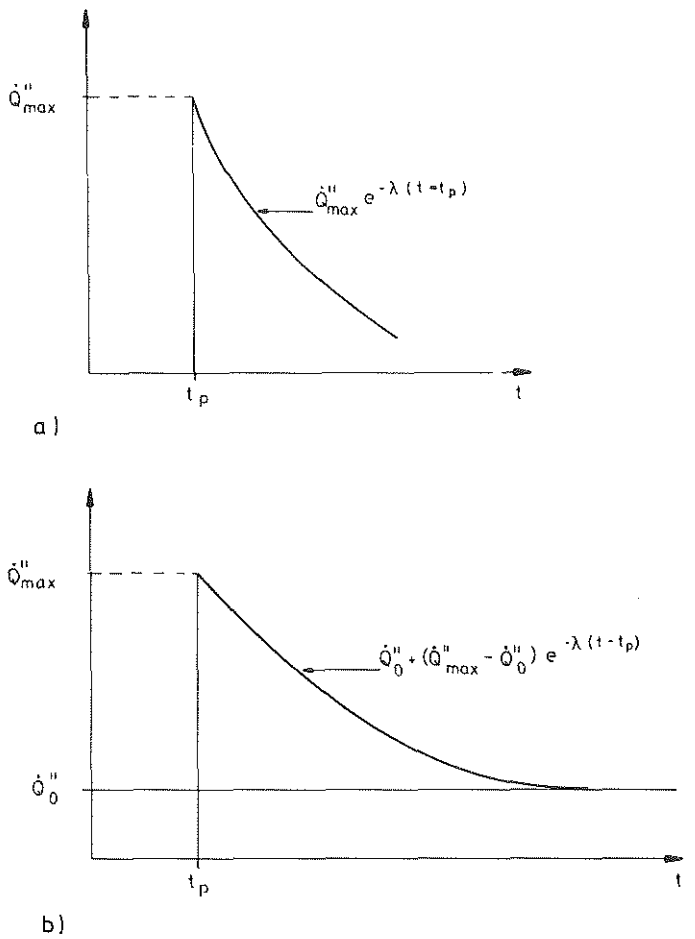

FIG. 4—*Principle for analytical approximation of experimental RHR curves.*

kW/m^2 level producing a RHR curve increasing in time and the 50-kW/m^2 level a decreasing curve. The remaining products may be characterized as char-forming cellulosic materials, in some cases with a thin surface cover.

Regression Analysis

Regression Equations

The derived $k\rho c$ values and RHR characteristics are to be inserted into the regression equations 8 and 9. We still have to determine the proper form of

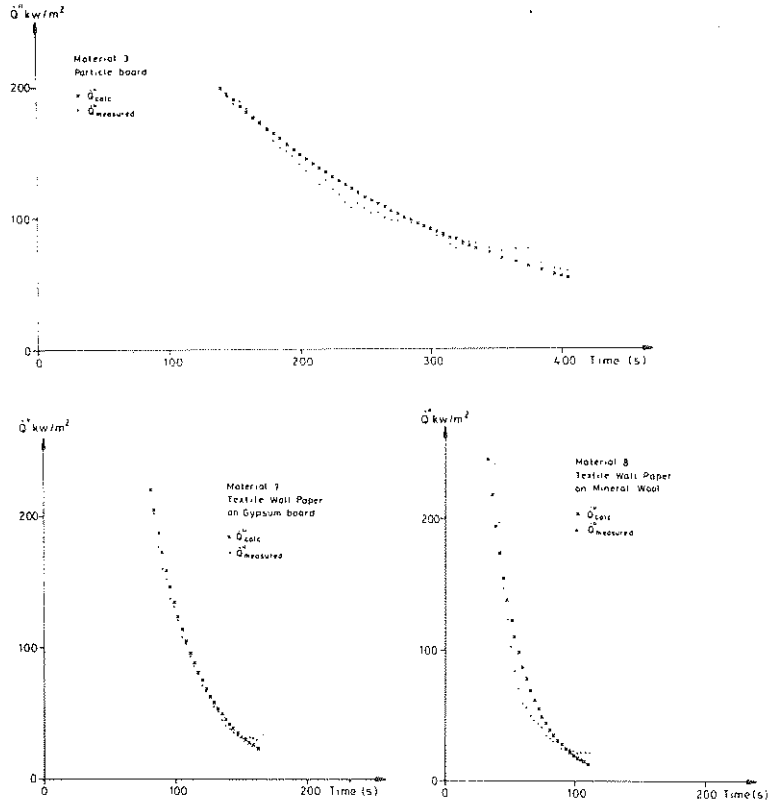

FIG. 5—*Experimental RHR curves and the corresponding analytical approximation, Eq 15*a.

$\dot{Q}''_{av}$. The simplest way of doing this would be to use a point estimate; that is, take $\dot{Q}''_{av} = \dot{Q}''(t_{av})$ with t_{av} equal to a fixed fraction of elapsed time t, say $0.5\,t$ or $0.75\,t$. The rational would be that $\dot{Q}_{ce}$ essentially is the product of two exponentials, where one, A_p, for most materials varies much faster than the other, $\dot{Q}''_{av}$, so that the time variation of the latter would be of little influence. Equation 9 would then be rewritten

$$\dot{Q}_{ce} = \alpha(e^{at} - 1)^{\beta}\dot{Q}''(t_{av}) \tag{16}$$

Another method would be to describe the interaction of flame spread and rate of heat release by a superposition, Duhamel-type integral.[3]

[3] Wickstrom, U., internal working memorandum, Swedish National Testing Institute, Borås, Sweden, Dec. 1983.

If we apply this method to our model and data, we obtain a simple expression for the integral (Fig. 6). We look at the situation at time $t_b = n\Delta t$ with pyrolyzing ceiling area $= A_p$. We have

$$\dot{Q}'' \sim e^{-\lambda t} \tag{17a}$$

$$A_p \sim e^{at} \quad \text{with} \quad a = h^2/k\rho c \tag{17b}$$

$$\Delta A_p \sim a e^{at} \Delta t \tag{17c}$$

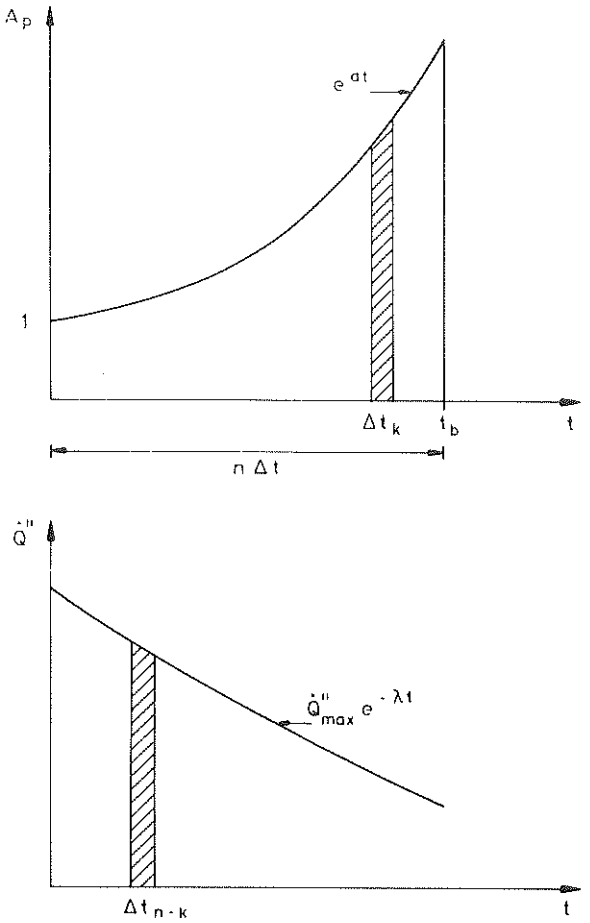

FIG. 6—*Principle behind superposition integral in Eq 19.*

For the infinitesimal area $\Delta A_{p,k}$ at time step k

$$\dot{Q}'' = \dot{Q}''(t_b - k\Delta t) = \dot{Q}''_{\max} e^{-\lambda(t_b - k\Delta t)} \tag{18}$$

and, in summation form, for the total pyrolyzing area A_p

$$\dot{Q}_{ce}(t = t_b) \sim \sum_{k=1}^{n} a e^{-\lambda(t_b - k\Delta t)} e^{ak\Delta t} \tag{19a}$$

or, in integral form,

$$\dot{Q}_{ce} \sim \int_0^{t_b} a e^{a\tau} \dot{Q}''_{\max} e^{-\lambda(t_b - \tau)} d\tau = \dot{Q}''_{\max} \frac{a}{a + \lambda} (e^{at} b - e^{-\lambda t} b) \tag{19b}$$

Equation 18 is a direct physical interpretation of the so-called Duhamel's formula expressing the response of a system to a general driving function $A_p(t)$ in terms of the experimentally accessible response [$\dot{Q}''(t)$ from Eq 15] of the system to a unit step function [*20*]. The methodology can be expanded to treat the case where the step response $\dot{Q}''(t)$ is a function of impressed flux instead of being linked to the constant value 30 kW/m^2. It has previously been used to correct heat release measurements from various small- and large-scale test apparatuses for the effect of inherent time delays in the measurement system [*21–23*].

Time Lag Compensation

When comparing calculated and measured energy release curves, time lags deriving from room-filling time, wall ignition time, transport time, and oxygen measuring instrument response time must be considered. The response of the measurement system to a unit step load may be written as [*24*]

$$U(t) = 1 - e^{-\gamma(t - t_d)} \tag{20}$$

if

$$t \geq t_d$$

$$U(t) = 0 \quad \text{for} \quad t < t_d$$

where

γ = characteristic of oxygen-measuring apparatus (the reciprocal of the "time constant"), and

t_d = delay or transport time of the combustion gases from burning zone to O_2 measuring cell.

If the true energy release rate from the full-scale test is written $\dot{Q}_{rs}$, the measured response $\dot{Q}_{mes}$ is given by the superposition integral

$$\dot{Q}_{mes} = \int_0^t U'(\tau)\dot{Q}_{rs}(t - \tau)d\tau \tag{21}$$

for $\tau \geq t_d$

Evaluation of the integral requires estimates of γ and t_d. For the type of oxygen analyzer involved, γ might be expected to be $\approx 0.25\ s^{-1}$ [24]. Experiments with furniture [4] where instantaneous mass loss rate can be compared with $\dot{Q}_{mes}$ indicate a transport time ≈ 15 s. Formulas for mass flow in plumes show a room-filling time, that is, the time it takes for the combustion gases to start flowing out of the doorway, to be in the order of 5 s for a 100 kW burner. Thus, t_d may be approximately 20 s. The form of the unit step load response means that parameters α and β in Eqs 16 and 19*b* cannot be determined by linear regression analysis. To avoid using nonlinear regression and the inherent computational difficulties, the following starting or calibration procedure was employed: $\dot{Q}_{rt}$ will be the sum of three terms: energy release from gas burner $\dot{Q}_{bu}$, from corner wall area $\dot{Q}_{co}$, and from ceiling material $\dot{Q}_{ce}$.

The sum of the first two parts is called $\dot{Q}_{\text{start}}$. If the burner is turned on at $t = 0$, a certain time t_{start} will elapse before the instruments register $\dot{Q}_{\text{start}}$. According to Eq 1*b*, another starting quantity is the initial pyrolyzing ceiling area, $A_{p,o}$, which is proportional to the initial ceiling flame area. This in turn is taken to be proportional to the heat energy stored in the unburnt fuel reaching the ceiling, $\dot{Q}_{uf}$. Regression Eqs 16 and 19*b* are then rewritten as, respectively,

$$\frac{\dot{Q}_{rt} - \dot{Q}_{\text{start}}}{\dot{Q}_{uf}} = \alpha(e^{at} - 1)^{\beta} \cdot \dot{Q}''(t_{av}) \tag{22a}$$

or

$$\frac{\dot{Q}_{rt} - \dot{Q}_{\text{start}}}{\dot{Q}_{uf}} = \alpha(e^{at} - e^{-\lambda t})^{\beta} \cdot \dot{Q}''_{\max} \cdot \frac{a}{a + \lambda} \tag{22b}$$

It should be observed that time t in Eq (22) will be measured from $t = t_{\text{start}}$. For most materials, the main component of t_{start} will be time to ignition of the wall corner lining material. In order to arrive at a practicable expression for t_{start}, a study was made of the correlation between t_{start} and the ignitability of the materials. The result was Fig. 7. It can be seen that with one exception, Material 13, t_{start} is closely approximated by the equation

$$t_{\text{start}} = t_{ig} + 5 \quad \text{(s)} \tag{23}$$

with t_{ig} measured at the 30 kW level.

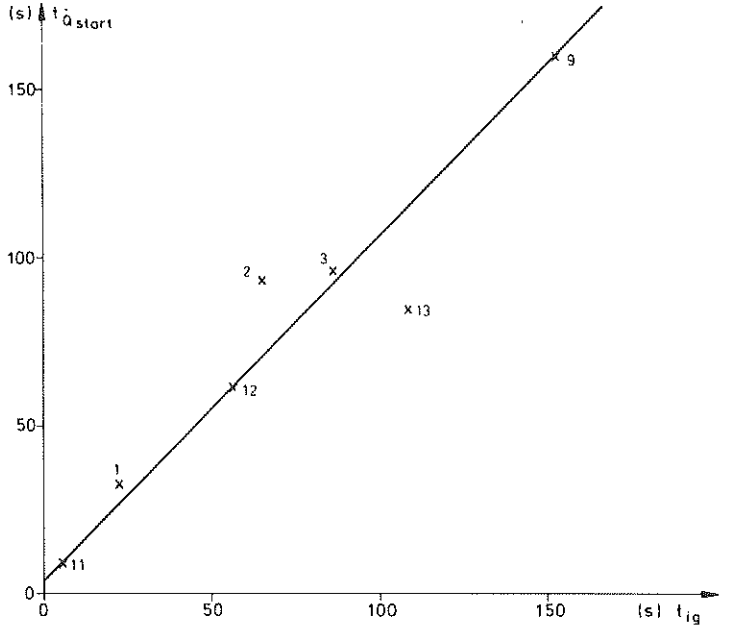

FIG. 7—*Relation between response time of room test RHR-measurement system and specimen ignitability time at 30 kW/m².*

It remains to determine $\dot{Q}_{uf} = \dot{Q}_{start}$ − wall flame combustion. A study of air entrainment into the wall plume showed that approximately 30 g O_2/s, corresponding to a heat release of 400 kW, is entrained into the wall flame. It is reasonable to assume that actual combustion before the plume hits the ceiling may be in the area of 60 to 150 kW. As the computations will be insensitive to choice of $\dot{Q}_{uf}$, mainly changing the value of the parameter α with a constant, it was decided to arbitrarily put

$$\dot{Q}_{uf} = \dot{Q}_{start} - 60 \tag{24}$$

Grouping of Materials

Looking at the full-scale tests, it was decided to divide the materials into two groups: one for which the depth of combustible material was thick enough so that no burning through would occur during time up to flashover (Materials 1-3, 9, 11-13), the other for which a thin combustible surface finish covered an incombustible baseboard (Materials 4-8). Material 10, polystyrene, was left outside the analysis.

Results of Parameter Estimation

If the logarithm is taken of both sides of Eq 22, the relations are transformed into first-order linear models where the parameters α' ($= f\alpha$) and β can be determined by linear regression. With $\dot{Q}_n$ describing the output from the full-scale tests, this procedure was followed for the seven materials 1-3, 9, 11-13, using a standard library regression program. Table 4 gives the value of α' and β plus the correlation coefficient r for the seven materials, using Eqs 22*a* and 22*b* as a base. When using Eq 22*a*, the value of t_{av} must be selected. Computations with $t_{av} = t/2$ and $t/4$ gave very similar results. In Table 4, $t_{av} = t/2$. The value of t_{start} was in each individual case taken directly from the full-scale measurements, *not* from Fig. 7. The value of the heat transfer coefficient h from ceiling flame or jet to lining material must be specified. As an initial approximation, a constant average value of 40 W/m^2 K was considered reasonable.

As can be observed, the regression model points to negligible difference between Eqs 22*a* and 22*b*. Consequently, for the remaining part of this paper we will concentrate further computations on Eq 22*a*. It should be remembered, however, that in Table 4 heat release rate is linked to a single curve for each material. A more correct model taking into account that impressed flux is variable during the full-scale experiments may indicate the need for choosing rate of heat release characteristics in a more detailed way.

The output of a general least square computer program usually includes standard error of the undetermined coefficients, standard error of the dependent variable, an analysis of the variance table, and the value of the (multiple) correlation coefficient r. A closer study of the computed residuals and confidence bounds have not been carried out as yet, but the values of correlation coefficient r in Table 4 indicate that the models of Eq 22 are reasonable. At the same time, there is a variation in α' and especially β between the materials which could invalidate use of Eq 22 in a design model. For this equation to be generally applicable for design purposes, variations in α' and β must have a limited influence on the final results. The next section will deal with this question.

TABLE 4—*Results from regression analysis.*

	Eq 22*a*			Eq 22*b*		
Material	α'	β	r	α'	β	r
1	−4.69	1.77	0.994	−4.78	1.78	0.994
2	−4.13	1.22	0.993	−4.16	1.22	0.993
3	−4.34	1.23	0.983	−4.40	1.23	0.982
9	−5.33	0.79	0.980	−5.52	0.75	0.973
11	−5.14	1.06	0.947	−5.14	1.04	0.944
12	−4.39	0.97	0.962	−4.42	0.93	0.958
13	−3.89	1.02	0.993	−3.91	1.01	0.993

Accuracy of Prediction Model

For the model according to Eq 22*a*, the average values and coefficients of variation for α' and β are

$$\bar{\alpha}' = -4.58 \tag{25a}$$

$$\sigma_{\alpha'}/\bar{\alpha}' = 0.13 \tag{25b}$$

$$\bar{\beta} = 1.15 \tag{26a}$$

$$\sigma_{\beta}/\bar{\beta} = 0.276 \tag{26b}$$

Seen in the light of the scatter inherent even in standard small-scale fire tests, the variability does not seem excessive. To find out its practical importance, the full-scale tests were recalculated on the basis of the values of α' and β given by expression 25*a* and 26*a*, that is, the average values. Furthermore, t_{start} was determined by Eq 24. Evidently this procedure is something of a circle proof that had to be accepted for lack of independent experimental data. The results can be seen in Figs. 8*a* to 8*g*. In substance, the agreement indicated the general validity of the derived parameters α and β. There are two essential deviations: Material 9, which behaved erratically in the small-scale tests [*17*], and Material 13. For the latter the difference is due to the fact that material takes much longer to ignite in the small-scale test than in the full-scale one (see Fig. 7). A recalculation using the correct ignition time for the room experiment showed a considerably better agreement (Fig. 8*g*).

Calculation of Complete Process

Knowing the parameters α and β and having estimates of the transport delay term t_d and oxygen instrument characteristic γ in Eq 20, the superposition integral Eq 21 can now be evaluated. An example is given in Fig. 1 for Material 3. For reasons of computational simplicity, the parameter β was taken as equal to 1.0. Figure 1 illustrates the practical applicability of the approach described in this paper.

Thin Surface Finishes on Noncombustible Baseboard

Five materials, Nos. 4–8, can be regarded as thin combustible surface finishes on noncombustible baseboard. In only one case, Material 8, was there a flashover during the initial period of 10 min with burner output equal to 100 kW. If we rewrite Eq 22*a* and replace t_{av} with t we get

$$\dot{Q}_{rf} = \dot{Q}_{start} + \dot{Q}_{inf} \cdot \alpha \cdot (e^{at} - 1)^{\beta} \cdot \dot{Q}''_{max} e^{-\lambda} \tag{22'}$$

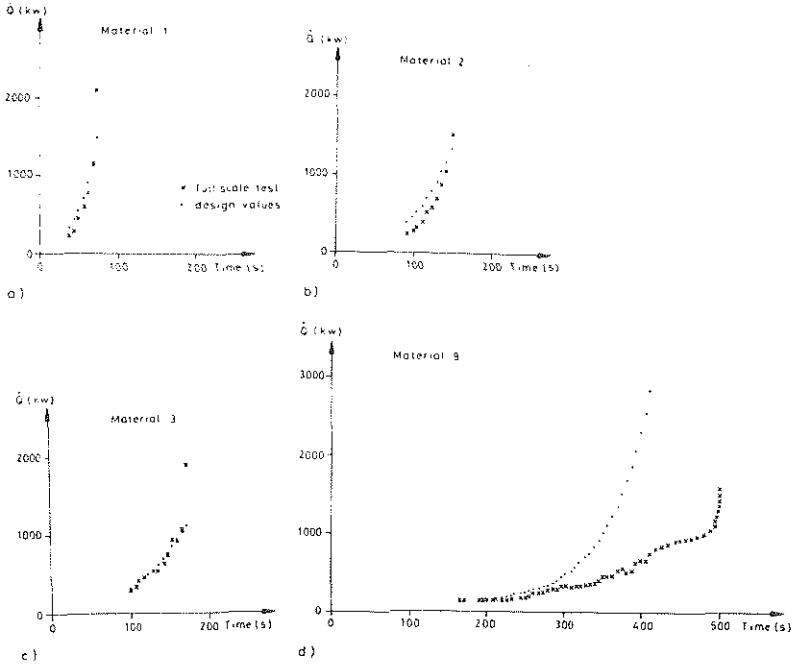

FIG. 8*a* to FIG. 8*g*—*Experimental RHR curves from room test (x) and design theory curves (·). The curve with ° in Fig. 8g denotes calculated values where response time equals experimental value.*

This expression will be bounded for all t only if

$$\beta a < \lambda \tag{27}$$

A look at Table 3 reveals that the condition is approximately fulfilled for Materials 4-7 but decidedly not for Material 8. The ratio $\beta a/\lambda$ is approximately 1.0, 0.72, 0.77, 0.72, and 9.7 for the five materials.

Equation 27 expresses the unbalance between the two competing processes: flame growth and decay in heat release rate. It should prove comparatively simple to incorporate the effects of partial burning through into Eq 21.[4]

It was demonstrated in Ref *13* that for thin materials a numerical simulation can be carried out, demonstrating the process when flame spreads over part of the ceiling, then recedes without causing flashover. The results were sensitive to choice of input data, and the procedure requires further exploration.

[4]Mitler, H., personal communication, June 1984.

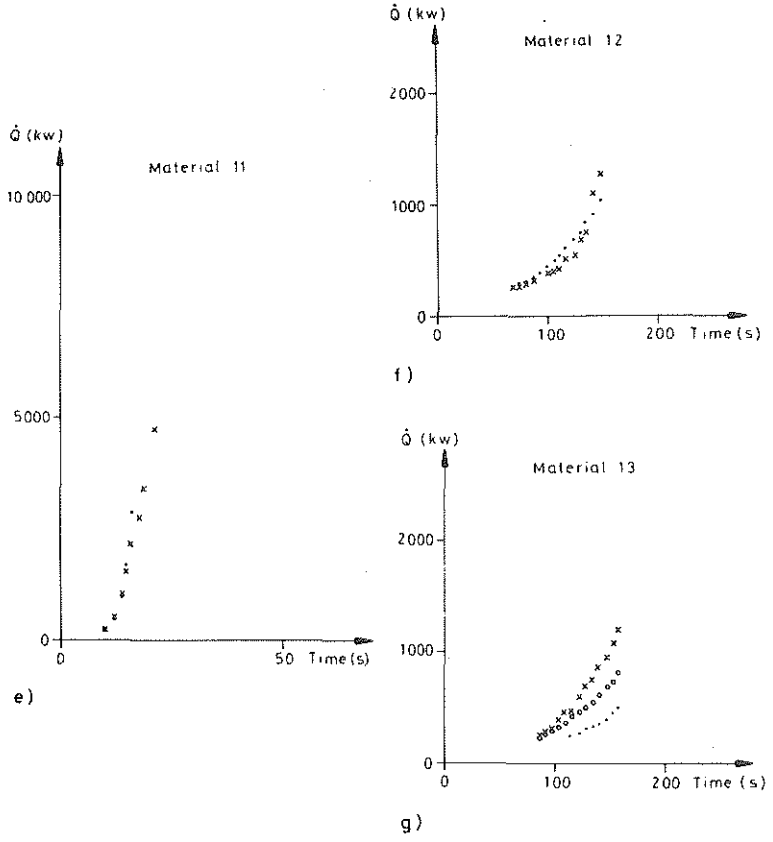

FIG. 8*a* to FIG. 8*g*—*Continued from previous page.*

Remarks on the Results

No sensitivity testing has so far been carried out with respect to the different assumptions and procedures just enumerated. It is likely that changes can be introduced into the analysis, leading to an improved consistency. As an example, putting the heat transfer coefficient equal to a constant is an oversimplification. It should be possible to describe h as a function of $\dot{Q}_{rl}(t)$ and in this way lessen the tendency of Eq 22*a* to underestimate $\dot{Q}_{rl}(t)$ when the test process is approaching flashover. Also, the effect of replacing the factor $h^2t/k\rho c$ with

TABLE 5—*Relative ranking of materials: Time, s, to reach 1 MW in room test.*

Material	Experiment	Design Equation
1	66	65
2	140	134
3	165	166
9	499	351
11	14	14
12	139	146
13	148	~205

$$\frac{h^2 t}{k\rho c}\,\frac{(T_f - T_u)^2}{(T_{ig} - T_u)^2}, \qquad (3b)$$

should be investigated.[4]

Finally, it should be pointed out that even if the predictive capability of the analysis in a quantitative sense may still be limited, it can be used qualitatively to rank materials. If we rank the seven materials with respect to the time it takes for the fire room test to reach 1 MW, the relative ranking is coincident in experiment and design theory (Table 5).

In summary, it is thought that a first step has been taken in the efforts to use results from small-scale flammability tests to rationally predict full-scale fire growth (for *one* specified scenario) and rank materials.

Further efforts should be directed firstly towards other fire scenarios, secondly towards code calibration studies. The sensitivity studies needed to derive confidence regions and safety factors can be based on the first order, second-moment statistical methods used in a number of engineering areas, for example, structural fire endurance [*24*].

Acknowledgment

The authors want to thank the other members of the project group for their valuable reviews. Berit Andersson is additionally thanked for her help in doing much of the computational work. To Henri Mitler, Center for Fire Research, National Bureau of Standards, goes our appreciation for a careful examination of an early version of this paper.

References

[*1*] "The Development of Tests for Measuring 'Reaction to Fire' of Building Materials," ISO Technical Report 3814, International Standards Organization, Geneva, Switzerland, 1975.

[*2*] "Fire Hazard and the Design and Use of Fire Tests," ISO Technical Report 6585, International Standards Organization, Geneva, Switzerland, 1979.

[*3*] Pettersson, O., "Fire Hazard and the Compartment Fire Growth Process—Outline of a

Swedish Joint Research Program," Report R80-5, Department of Structural Mechanics, Lunds Institute of Technology, Lund, Sweden, 1980.

[4] Wickström, U., Sundström, B., and Holmstedt, G., *Fire Safety Journal*, Vol. 5, 1983, pp. 191-197.

[5] "Proposed Method for Room Fire Test of Wall and Ceiling Materials and Assemblies," *Annual Book of ASTM Standards*, Pt. 18, ASTM, Philadelphia, Nov. 1982.

[6] Orloff, L., de Ris, J., and Markstein, G. M., "Upward Turbulent Fire Spread and Burning of Fuel Surfaces," 15th Symposium (International) on Combustion, 1975.

[7] Fernandez-Pello, A. C. and Mao, C. P., *Combustion Science and Technology*, Vol. 26, Gordon and Breach Science Publishers, London, England, 1981, pp. 147-155.

[8] Parker, W. J., "An Assessment of Correlations Between Laboratory and Full-Scale Experiments for the FAA Aircraft Fire Safety Program, Part 3: ASTM E 84," NBSIR 82-2564, Center for Fire Research, Washington, DC, August 1982.

[9] Quintiere, J., "An Assessment of Correlations between Laboratory and Full-Scale Experiments for the FAA Aircraft Fire Safety Program, Part 2: Rate of Energy Release in Fire," NBSIR 82-2536, Center for Fire Research, Washington, DC, July 1982.

[10] Harkleroad, M., Quintiere, J., and Walton, W., "Radiative Ignition and Opposed Flow Flame Spread Measurements in Materials," Report No. DOT/FAA-CT-83/28, U.S. Department of Transportation, FAA Technical Center, Atlantic City Airport, N.J., August 1983.

[11] Östman, B., "Ignitability as Proposed by the International Standards Organization Compared with Some European Fire Tests for Building Panels," *Fire and Materials*, Vol. 5, No. 4, 1981.

[12] Heselden, A., "Notes on the Meaning and Use of the ISO Ignitability Test," ISO/TC92/WG2 N33, International Standards Organization, Geneva, Switzerland, Sept. 1981.

[13] Magnusson, S. E. and Sundström, B., "Modelling of Room Fire Growth—Combustible Lining Materials," LUTVDG/(TVBB-3019), Division of Building Fire Safety and Technology, Lund, Sweden, Feb. 1984.

[14] Atreya, A., "Pyrolysis, Ignition and Fire Spread on Horizontal Surfaces of Wood," Thesis, Appendix E, Harvard University, Cambridge, MA, May 1983.

[15] Blomqvist, J., "RHR of Building Materials—Experiments with an OSU-Apparatus Using Oxygen Consumption," Report LUTVDG/(TVBB-3017), Division of Building Fire Safety and Technology, Lund University, Lund, Sweden, 1983.

[16] Sensenig, D. L., "An Oxygen Consumption Method for Determining the Contribution of Interior Wall Finishes to Room Fires," NBS Technical Note 1128, National Bureau of Standards, Washington, DC, 1980.

[17] Svensson, G., and Östman, B., "Rate of Heat Release by Oxygen Consumption Testing of Building Materials," Meddelande Serie A Nr 812, Swedish Institute for Wood Research, Stockholm, Feb. 1983.

[18] Babrauskas, V., "Development of the Cone Calorimeter—A Bench-Scale Heat Release Rate Apparatus Based on Oxygen Consumption," NBSIR 82-2611, National Bureau of Standards, Washington, DC, 1982.

[19] Delichatsios, M. A. and de Ris, J., "An Analytical Model for the Pyrolysis of Charring Materials," presented at the CIB W14 meeting in Borås, Sweden, May 1983, Factory Mutual Research, Norwood, MA.

[20] Wylie, C. R. in *Advanced Engineering Mathematics*, 4th ed., McGraw-Hill, New York, 1975, p. 313.

[21] Evans, D. D. and Breden, L. H., "A Numerical Technique to Correct Heat Release Rate Calorimetry Data for Apparatus Time Delay," NBSIR 77-1302, Center for Fire Research, Washington, DC, Nov. 1977.

[22] Vandevelde, P., "An Evaluation of Heat Release Criteria in Reaction-to-Fire Tests," *Fire and Materials*, Vol. 4, No. 3, 1980.

[23] Babrauskas, V., Lawson, J. R., Walton, W. D., and Twilley, W. H., "Upholstered Furniture Heat Release Rates Measured with a Furniture Calorimeter," NBSIR 82-2604, Center for Fire Research, Washington, DC, Dec. 1982.

[24] Magnusson, S. E., "Probabilistic Analysis of Fire Exposed Steel Structures," Bulletin 27, Division of Structural Mechanics and Concrete Construction, Lund University, Sweden, 1974.